Low-Spin Heme b_3 in the Catalytic Center of Nitric Oxide Reductase from *Pseudomonas nautica*

Cristina G. Timóteo,[†] Alice S. Pereira,*[,†] Carlos E. Martins,[†] Sunil G. Naik,[‡] Américo G. Duarte,[†] José J. G. Moura,[†] Pedro Tavares,[†] Boi Hanh Huynh,[‡] and Isabel Moura*[,†]

[†]Requimte, Centro de Química Fina e Biotecnologia, Departamento de Química, Faculdade de Ciências e Tecnologia, Universidade Nova de Lisboa, Quinta da Torre, 2829-516 Monte de Caparica, Portugal

[‡]Department of Physics, Emory University, Atlanta, Georgia 30322, United States

S *Supporting Information*

ABSTRACT: Respiratory nitric oxide reductase (NOR) was purified from membrane extract of *Pseudomonas (Ps.) nautica* cells to homogeneity as judged by polyacrylamide gel electrophoresis. The purified protein is a heterodimer with subunits of molecular masses of 54 and 18 kDa. The gene encoding both subunits was cloned and sequenced. The amino acid sequence shows strong homology with enzymes of the cNOR class. Iron/ heme determinations show that one heme c is present in the small subunit (NORC) and that approximately two heme b and one non-heme iron are associated with the large subunit

(NORB), in agreement with the available data for enzymes of the cNOR class. Mössbauer characterization of the as-purified, ascorbate-reduced, and dithionite-reduced enzyme confirms the presence of three heme groups (the catalytic heme b_3 and the electron transfer heme b and heme c) and one redox-active non-heme Fe (Fe_B). Consistent with results obtained for other cNORs, heme c and heme b in *Ps. nautica* cNOR were found to be low-spin while Fe_B was found to be high-spin. Unexpectedly, as opposed to the presumed high-spin state for heme b_3, the Mössbauer data demonstrate unambiguously that heme b_3 is, in fact, low-spin in both ferric and ferrous states, suggesting that heme b_3 is six-coordinated regardless of its oxidation state. EPR spectroscopic measurements of the as-purified enzyme show resonances at the $g \sim 6$ and $g \sim 2-3$ regions very similar to those reported previously for other cNORs. The signals at $g = 3.60, 2.99, 2.26,$ and 1.43 are attributed to the two charge-transfer low-spin ferric heme c and heme b. Previously, resonances at the $g \sim 6$ region were assigned to a small quantity of uncoupled high-spin Fe^{III} heme b_3. This assignment is now questionable because heme b_3 is low-spin. On the basis of our spectroscopic data, we argue that the $g = 6.34$ signal is likely arising from a spin–spin coupled binuclear center comprising the low-spin Fe^{III} heme b_3 and the high-spin Fe_B^{III}. Activity assays performed under various reducing conditions indicate that heme b_3 has to be reduced for the enzyme to be active. But, from an energetic point of view, the formation of a ferrous heme-NO as an initial reaction intermediate for NO reduction is disfavored because heme $[FeNO]^7$ is a stable product. We suspect that the presence of a sixth ligand in the Fe^{II}-heme b_3 may weaken its affinity for NO and thus promotes, in the first catalytic step, binding of NO at the Fe_B^{II} site. The function of heme b_3 would then be to orient the Fe_B-bound NO molecules for the formation of the N–N bond and to provide reducing equivalents for NO reduction.
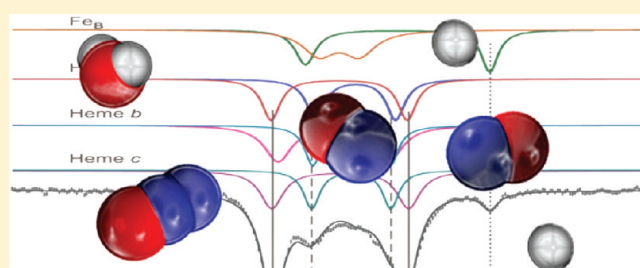
$\mathbf{D}$enitrifying bacteria can be found in a wide variety of environments ranging from streams, soils, to human intestines. *Ps. nautica* 617 is a halofile bacterium found in marine sediments contaminated with effluents from oil refineries.[1,2] It is able to reduce nitrate to dinitrogen by utilizing the catalytic functions of four specific enzymes:[3] The Mo-pterin containing nitrate reductase, the cytochrome cd_1 nitrite reductase, the cytochrome bc complex nitric oxide reductase, and the Cu-containing nitrous oxide reductase. The nitrate reductase, cytochrome cd_1, and nitrous oxide reductase from *Ps. nautica* have been subjected to extensive biochemical and structural studies,[4–7] while detailed characterization of nitric oxide reductase (NOR) from *Ps. nautica* has not been reported.

There are three classes of NOR identified in bacteria, all membrane bound. The first class, called cNOR, uses a soluble cytochrome c or a cupredoxin as its electron donor, whereas the two other classes, qNOR and qCuNOR, are quinol oxidases. The cNOR's are composed of two subunits: a small subunit (NORC, $\sim$17 kDa) that contains a c-type heme and a large subunit (NORB, $\sim$56 kDa) that contains two b-type hemes and a non-heme iron. Enzymes belonging to this class have been isolated from four denitrifying bacteria: *Ps. stutzeri*,[8,9] *Paracoccus (Pa.)*

denitrificans,[10,11] *Halomonas (H.) halodenitrificans*,[12,13] and more recently *Ps. aeruginosa*.[14] The enzymes of the qNOR class consist of only one subunit of 84.5 kDa. Similar to the NORB subunit of cNOR, each molecule of qNOR contains two *b*-type hemes and one non-heme iron. With the exception of the qNOR isolated from the denitrifying bacteria *Ralstonia eutropha*,[15] all other purified qNOR's reported so far were identified in pathogenic microorganisms lacking the other denitrifying enzymes.[16,17] The qCuNOR has been isolated from the Gram-positive denitrifying *Bacillus azotoformans*.[18] It is a heterodimer, composed of a small subunit of 16 kDa containing a Cu_A center and a large subunit of 57 kDa containing two *b*-type hemes and a non-heme iron center, similar to those in qNOR and in NORB of cNOR.

The NORs of all three classes catalyze the two-electron reduction of nitric oxide to nitrous oxide, a reaction that involves the formation of a N—N bond:

$$2NO + 2e^- + 2H^+ \rightarrow N_2O + H_2O$$

Biochemical and spectroscopic investigations of cNORs, together with site-directed mutagenesis studies, have provided evidence for a binuclear catalytic site, comprising a heme *b* (heme b_3) and a non-heme iron center (Fe_B).[19−21] In the resting state of the enzyme (oxidized form), both Fe sites are suggested to be high-spin ferric and antiferromagnetically coupled, most probably, through a μ-oxo bridge,[22] resulting in a diamagnetic ground state and consequently EPR silent. The mechanism of NO reduction remains a subject of intense interest and has been reviewed recently.[23−26] Currently two alternative mechanisms are being considered, namely, the *cis* and *trans* mechanism. In the *cis* mechanism, one of the two iron sites of the binuclear center binds both NO molecules, and the other Fe site plays the role of electron transfer and/or assist in abstracting the O atom from one of the NO molecules. In the *trans* mechanism, one NO molecule is bound to each one of the iron sites of the binuclear center. Ultrarapid freeze quench EPR studies under single turnover conditions showed simultaneous appearance of EPR signals that are characteristics of ferrous heme—NO and non-heme ferrous—NO complexes at 0.5 ms after introduction of NO,[14] providing evidence for the proposed *trans* mechanism. A recent spectroscopic study of a functional model complex also shows a reaction intermediate that exhibits both a $S = 3/2$ $[Fe_BNO]^7$ and a $S = 1/2$ heme Fe(II)—NO EPR signal, supporting the *trans* mechanism.[27] On the other hand, ferrous heme—NO complexes are highly stable, making it improbable for ferrous heme—NO to be a reaction intermediate. Also, a redox titration study of the *Pa. denitrificans* cNOR shows that the midpoint redox potential of heme b_3 is more than 200 mV lower than that of Fe_B,[28] indicating the presence of a thermodynamic barrier to prevent the reduction of heme b_3 and thus avoid the formation of a highly stable, probably inhibitory, ferrous heme b_3—NO complex. The presence of such a thermodynamic barrier has led to the proposal that the three-electron-reduced cNOR with an oxidized heme b_3 is the active form of the enzyme.[28] In support of this proposal, studies of cyanide binding to various redox states of the enzyme indicated that affinity for CN^- for the three-electron-reduced state is 1000-fold higher than that for the fully reduced or oxidized state.[29] But, interestingly, more recent studies with *H. halodenitrificans* cNOR[12] showed that NO can bind to both heme b_3 and Fe_B in their oxidized as well as reduced states and that the key determining factor in preventing NO binding to the binuclear center is the presence of the μ-oxo bridge. Either a

weakening or a rupturing of the oxo-bridge would permit the binding of NO irrespective of the redox state of the heme b_3—Fe_B center. Here we report a detailed biochemical and spectroscopic characterization of cNOR isolated from the denitrifying bacterium *Ps. nautica*. In contrast to previously assumed high-spin state for heme b_3 in cNORs isolated from other organisms, our results indicate that, for *Ps. nautica* cNOR, heme b_3 is low-spin in both oxidized and reduced states and that heme b_3 has to be reduced for the enzyme to be active.

■ EXPERIMENTAL PROCEDURES

Cell Growth and NOR Purification. *Pseudomonas nautica* 617 cells were grown as described in Prudêncio et al.[6] For [57]Fe growth, $FeSO_4$ was replaced by the [57]Fe isotope salt. Cells were harvested by centrifugation at the end of the stationary phase. The yield in wet weight was 1 g of cells per liter of culture medium. Cells were ressuspended in 100 mM Tris-HCl pH = 7 buffer and disrupted on a French Press. The crude extract was centrifuged at 8000g for 20 min to separate the intact cells and only then ultracentrifuged twice at 125000g for 90 min to recover the membrane fraction, which was frozen at −80 °C. Membranes were washed as described in Girsh et al.,[19] except for the sonication step that was done in 500 mL portions, in four cycles of 10 min in ice. All ultracentrifugation steps were performed at 180000g for 90 min. Purification of nitric oxide reductase was carried out at 4 °C, following a modified procedure from the one described in Girsh et al.[19] Proteolysis inhibitors (1 mM PMSF and 10 mM benzamidine) were added to the supernatant of the extraction with 0.6% of DDM. The percentage of detergent used was judged to be effective as no significant NOR activity remained in the membrane fraction. This supernatant was applied to a DEAE-Biogel A column (Bio-Rad, 5.5 × 25.5 cm, 140 mL of resin per gram of protein) equilibrated with 50 mM Tris-HCl pH = 8, 0.02% DDM, 0.01% (v/v) 2-phenylethanol. The column was washed with 460 mL of the same buffer. A linear gradient between 0 and 500 mM NaCl was used, with a total volume of 2 L. The presence of NOR was assessed by activity assays and UV/vis spectroscopy. The fractions with specific activity higher than 40%, eluted between 250 and 400 mM NaCl, were pooled. After a concentration step in a Diaflo apparatus (Amicon) with a YM30 membrane, the buffer was exchanged to 10 mM potassium phosphate buffer (KPB) pH 7, 400 mM NaCl, and the fraction was frozen in 340 mg aliquots of protein. Each aliquot was then further purified in a Macro-prep ceramic hydroxyapatite CHT-I 20 μm column (Bio-Rad, 2.6 × 27 cm) coupled to a ÄKTA basic HPLC system (Amersham Biosciences). A linear gradient was applied using NaCl (0.4−0 M) and potassium phosphate buffer (KPB, 0.010−1.50 M), pH 7, with a flow of 2 mL/min for 3 h. A second chromatographic step was performed using a Bio-Scale CHT20-I prepacked column with the same gradient. NOR was eluted between 300 and 350 mM KPB. For the ceramic hydroxyapatite columns, the concentration of detergent had to be increased both in the fraction injected (to 0.1%) and in the buffers (to 0.05%) in order to prevent further spreading of the protein in the column. In these last steps of purification, NOR containing fractions that have absorbance ratio between 410 and 280 nm higher than 1 were pooled. Purity of the isolated enzyme was verified by tricine SDS-PAGE electrophoresis. The protein was then concentrated and the buffer exchanged to 100 mM KPB pH 7, 0.02% dodecyl maltoside, 0.01% 2-phenylethanol.

Tricine Sodium Dodecyl Sulfate Electrophoresis. SDS-PAGE was performed using a method developed by Shagger and von Jagow,[30] which uses tricine instead of glicine buffer and has the advantage of conveying the same degree of separation as in the Laemmli method with lower acrylamide concentrations. To avoid smearing of the NOR bands and aggregation, samples were incubated at 40 °C for 30 min before loading.

Spectroscopic Methods. UV/vis spectra were recorded in a Shimadzu UV-265 split-beam spectrophotometer connected to an IBM PC compatible computer. Low-temperature EPR measurements were performed in an X-band Bruker EMX spectrometer equipped with an Oxford Instruments liquid helium flow cryostat. Weak-field Mössbauer spectra were recorded on a spectrometer equipped with a Janis 8DT variable-temperature cryostat. The Mössbauer spectrometer operates at a constant acceleration mode in transmission geometry. The zero velocity refers to the centroid of a room temperature spectrum of a metallic iron foil. Analysis of the Mössbauer spectra was performed with the program WMOSS (SEE Co.).

Enzymatic Assay. NO reductase activity was measured with an ISO-NO Mark II electrode with a 2 mm sensor in an appropriate reaction vessel (World Precision Instruments). NO aqueous solution, 100 μM at 20 °C,[19] was prepared from a 5% NO/95% He mixture (Air liquide). The NO/He mixture was previously washed by bubbling in a 5 M KOH solution and through nonbuffered water, at pH 3, to prevent NO_2^- formation. The reaction vessel, with the electrode fitted on top, was degassed prior to addition of solution. Degassed solution of 20 mM KPB, pH 6, 0.02% (w/v) DDM containing the electron donor was introduced. NO aqueous solution was then added, and the assay was initiated by enzyme addition (70 nM final protein concentration). ISO-NO Mark II electrode was coupled to a Quad-16/EFA-400, and data acquisition/treatment was performed by Data-Trax Data Acquisition software (World Precision Instruments). Different cytochromes from *Ps. nautica*, purified as described by Saraiva et al.,[31,32] were used as electron donors, each at a concentration of 3 μM in the assay solution.

Protein and Metals Determination. Protein determination was performed using the BCA method (Sigma) or by the Lowry method[33] using bovine heart cytochrome c as standard. Total iron content was determined by inductive coupled plasma emission analysis. Heme b and c content was determined by the pyridine hemocromogen method. The results were analyzed according to Berry and Trumpower.[34] Non-heme iron content was determined by the TPTZ method.[35] Amino acid analysis was performed as described by Moore et al.[36] after a 24 or 48 h hydrolysis with 6 N HCl at 110 °C with a Pharmacia Alpha Plus Aminoacid analyzer.

NOR Gene Coding Sequence Determination. *Ps. nautica* 617 cells were grown for 16 h, at 30 °C, 220 rpm, in the absence of nitrate. Genomic DNA was isolated using a standard CTAB extraction protocol.[37] To obtain the sequence of the NOR-encoding gene, a first PCR was performed, using degenerate primers, designed by comparison of known NORB protein sequences. PCR was performed in a thermal cycler (Biometra). A product of ~980 bp was obtained, purified by gel extraction using the QIAquick Gel Extraction Kit (QIAGEN) and ligated into the pGEM-TEasy commercial vector (Promega) according to the manufacturer's instructions. The ligation product was used to transform *Epicurian coli* XL1-Blue competent cells (Stratagene). Positive clones (white colonies) were grown overnight in Luria Broth medium with 100 μg/mL ampicilin at 37 °C. Plasmid DNA was isolated and sequenced in a Amersham Pharmacia Biosciences ALF Express II automated sequencer. The remaining sequence of NORB subunit and the sequence of the NORC subunit were obtained applying the Universal Genome Walker Kit (Clontech) according to the manufacturer's instructions. All primers were synthesized by Sigma-Genosys.

Redoxt Titration. Redox titrations were carried out in an anaerobic chamber. The redox potential was measured directly in the cell using a combined silver/silver chloride and platinum electrode (Crison) calibrated with quinhydrone at controlled pH. Several different dye mediators at 0.10 μM (anthraquinone-2-sulfonate, 2-hydroxy-1,4-naphthoquinone, phenazine, duroquinone, 5′-hydroxy-1,4-naphthoquinone, 1,4-naphthoquinone, phenazine metasulfate, 1,2-naphthoquinone, tetramethyl-*p*-phenylenediamine, 1,2-naphthoquinone-4-sulfonic acid, potassium ferricyanide, phenazine ethasulfate, and 2,5-dimethylbenzoquinone) were added to the protein sample, selected in order to minimize their interference at wavelengths of interest. The reaction mixture was buffered with the mix described above. Reduction was accomplished by adding aliquots of concentrated solutions (15−25 mM) of sodium ascorbate or dithionite. Visible spectra (395−900 nm) were monitored with a J&M Tidas diode array spectrophotometer.

■ RESULTS

General Biochemical and Physical Properties. The DNA sequence of the gene that codifies *Ps. nautica* cNOR was determined (see Figure S1, Supporting Information). Figure 1 compares the *Ps. nautica* cNOR primary sequence, deduced from the gene sequence, with those of other bacterial cNORs. The histidine residues that have been identified as ligands of the heme iron and non-heme iron atoms (H53 and H342 for heme b; H340 for heme b_3; H200, 251, and 252 for Fe_B) and the catalytically essential glutamate residues (E128, E131, E204, E208, and E273)[38−41] are all conserved in *Ps. nautica* cNOR. In addition, two other histidine (H322 and H332) and five other glutamate residues (E75, E76, E80, E228, and E231) are also conserved. From the deduced amino acid composition and Fe cofactor content (one heme c in NORC; two heme b moieties and a non-heme Fe in NORB), molecular masses of 17 590 and 54 380 Da were calculated respectively for *Ps. nautica* NORC and NORB subunits. On SDS-PAGE gel, purified *Ps. nautica* cNOR shows two bands with apparent molecular masses of 17 kDa (NORC subunit) and 36 kDa (NORB subunit). The apparent molecular mass of NORC subunit determined from SDS-PAGE is similar to that calculated from its gene-coding primary sequence. The apparent molecular mass of NORB determined from SDS-PAGE is substantially different from that deduced from the amino acid composition, however. This discrepancy had been reported for other cNORs and was attributed to the hydrophobic character of NORB.[9,13,19] Heme staining methodology revealed that only the low molecular weight band (i.e., NORC subunit) had a covalently ligated heme. A total iron content of 3.5 ± 0.5 Fe/cNOR molecule was obtained by plasma emission analysis. Calcium content was determined to be 0.7 ± 0.2 Ca/cNOR. No other transition metal was detected. Values of 1.0 ± 0.1 Fe and 1.7 ± 0.2 Fe per NORB subunit were obtained for non-heme iron and heme b, respectively, while a value of 1.0 ± 0.1 Fe/NORC subunit was obtained for heme c, consistent with a cofactor stoichiometry of 1:2:1 for heme c:heme b:non-heme iron.

A

```
              1         10        20        30        40        50        60        70
Ps.nautica          MAERFTKSMARNIYLGGSAFFVLLFLALTFDTQLRAMPERDNRDELTEQVVRGKHLWEENNCVGCHSIRG
Ps.aeruginosa       MSETFTKGMARNIYFGGSVFFILLFLALTYHTEK.TLPERTNEAAMSAAVVRGKLVWEQNNCVGCHTLLG
Ps.stutzeri         MSETFTKGMARNIYFGGSVFFFLVFLGLTYHTEQ.TFPERTNESEMTEAVVRGKEVWENNNCIGCHSLLG
Pa.denitrificans    MSEIMTKNMARNVFYGGSIFFILIFGALTVHSHIYARTKAVDESQLTPSVVEGKHIWERNACIDCHTLLG
Pa.halodenitrificans MADGLTKSAARNIFYGGSLFFFLLFAALTAHSHWYMVNKSTDNEGLTESVVAGKHIWEKNMCINCHSIMG

                       80        90        100       110       120       130
Ps.nautica          EGAYFAPELANVFDRRGGG.DTEVFKAYMKAWMNAMPTNIPGRRQMPDFNLSDSEVEDLAAFLEWTSKID
Ps.aeruginosa       EGAYFAPELGNVVGRRGG...EEGFNTFLQAWMNIQPLNVPGRRAMPQFHLSEGQVDDLAEFLKWSSKID
Ps.stutzeri         EGAYFAPELGNVFVRRGG...EETFKPFLHAWMKAQPLGAPGRRAMPQFNLSEQQVDDMAEFLKWTSKID
Pa.denitrificans    EGAYFAPELGNVMKRWGVQDDPDSAFETLKGWMESMPTGIEGRRQMPRFDLTDEEFRALSDFLLWTGTIN
Pa.halodenitrificans EGAYFAPELSNVWERYGGHQNPEAARAGLAAWIRAQPLGTQGRRQMPAYDFTDEEMSSLIDFLEWTDGID

                       140
Ps.nautica          DNGWPPNIEG
Ps.aeruginosa       TNQWPPNKEG
Ps.stutzeri         TNDWPPNKEG
Pa.denitrificans    TQNWPPNDAG
Pa.halodenitrificans DQDWPPHPAG
```

B

```
              1         10        20        30        40        50        60
Ps.nautica          .......MKYESQRVAMPYFIFALILFAGCIVFGLILGLQYVVGDFLFPEIPFNVARMVHTNLLIVWLLF
Ps.stutzeri         MSSFNPHLKFQSQAVAKPYFVFALILFVGCVLFGLIMGLQYVVGDFLFPLLPFNVARMVHTNLLIVWLLF
Ps.aeruginosa       MMSPNGSLKFASQAVAKPYFVFALILFVGCILFGLIMGLQYVVGDFLFPAIPFNVARMVHTNLLIVWLLF
Pa.denititrificans  .......MRYHSQRIAYAYLLVAMVFEAVQVTIGLIMGWIYYSPNELSELLPFNIARMLHTNSLVVWLLL
Pa.halodenitrificans .......MKYETQKVALPFLMVAMAFFALQIVFGLLAAAVYVWPNFMAEAMPFNIMRASHTNLLIVWLLI

                       70        80        90        100       110       120       130
Ps.nautica          GFMGATYYMVPEEAQTELHSPLLAWILFWVFAAAGTLTILGYLFVDYATLAEVTMNKLLPTMGREFLEQP
Ps.stutzeri         GFMGAAYYLIPEESDCELHSPKLAIILFWVFAAAGVLTILGYLFVPYAALAEMTRNDLLPTMGREFLEQP
Ps.aeruginosa       GFMGAAYYLVPEESDCELYSPKLAWILFWVFAAAGVLTILGYLLVPYAGLARLTGNELWPTMGREFLEQP
Pa.denititrificans  GFFCATYYILPEEAERELHSPLLAWIQLGIFVLGTAGVVVTYLFDLFHGHWLLGK......EGREFLEQP
Pa.halodenitrificans GFMGSTYYLMPEEAERELHSPTIAYIQLAIFAFAGAAALVGYQFGIHE.............GREFLEQP

                       140       150       160       170       180       190       200
Ps.nautica          TITKIGIAVVVVAPLYNIAMTALKGRKTVVNIVLITGLVGLAVLWLFSFYNPGNLATDKYFWWFVVHLWV
Ps.stutzeri         TITKIGIVVVALGFLYNIGMTMLKGRKTVVSTVMMTGLIGLAVFPLFAFYNPENLSRDKFYWWFVVHLWV
Ps.aeruginosa       TISKAGIVIVALGFLFNVGMTVLRGRKTAISMVLMTGLIGLALLFLFSFYNPENLTRDKFYWWWVVHLWV
Pa.denititrificans  KWVVKLGIAVAAVILFMYNVSMTALKGRRTAVTNVLLMGLWGLVLLWLFAFYNPANLVLDKQYWWWVIHLWV
Pa.halodenitrificans FWVKLLITISFLMFLFNTSMTLPKGRKTAINMVLMLGLWLAAVFWLFAFYNPSNLAVDKLYWWWVVHLWV

                       210       220       230       240       250       260       270
Ps.nautica          EGVWELIMGAILAYVLIKLTGVDREVIEKWLYVIIAMALITCIIGTGHHFFWIGPPEYWLWLGSVFSALE
Ps.stutzeri         EGVWELIMGAMLAFVLIKVTGVDREVIEKWLYVIIAMALITGIIGTGHHFFWIGAPTVWLWVGSIFSALE
Ps.aeruginosa       EGVWELIMGAILAFVLVKITGVDREVIEKWLYVIIAMALISGIIGTGHHYFWIGVPGYWLWLGSVFSALE
Pa.denititrificans  EGVWELIMAAILAFLMLKLTGVDREVIEKWLYVIVATALFSGILGTGHHYYWIGLPAYWQWIGSIFSSFE
Pa.halodenitrificans EGVWELIMASLLGYLLIKMTGVDREVIEKWLYVIVGLALFSGLLGTGHHYYWIGAPSYWQPIGSIFSTLE

                       280       290       300       310       320       330       340
Ps.nautica          PLPFFMVVVFAFNMINRRRR.NHPNKAAMLWAMGTTVMAFLGAGVWGFLHTLAPVNWYTHGSQITAAHGH
Ps.stutzeri         PLPFFAMVLFALNMVNRRRR.EHPNKAASLWAIGTTVTAFLGAGVWGFMHTLAPVNYYTHGSQLTAAHGH
Ps.aeruginosa       PLPFFALVLFAFNTINRRRRRDYPNRAVALWAMGTTVMAFLGAGVWGFMHTLAPVNYYTHGTQLTAAHGH
Pa.denititrificans  IVPFFAMMSFAFVMVWKGRR.DHPNKAALVWSLGCTVLAFFGAGVWGFLHTLHGVNYYTHGTQITAAHGH
Pa.halodenitrificans VLPFFAMVIFAFTMFWKGSR.NHPNKAAMLWALGCPTMAFFGAGVWGFMHTLHWVNYYSHGTQVTAAHGH

                       350       360       370       380       390       400       410
Ps.nautica          MAFYGAYVMIVLTIISYAMPIMRGRPYGNSNTAQIVEMWGFWLMTISMVFITLPLTAAGVLQVWLQRIPE
Ps.stutzeri         LAFYGAYAMIVMTMISYAMPRLRGLGEAPDARAQRIEVWGFWLMTISMIAITLFLTAAGVVQIWLQRIPA
Ps.aeruginosa       MAFYGAYAMIVMTIISYAMPRLRGIGEAMDNRSQVLEMWGFWLMTVAMVFITLPLSAAGVLQVWLQRMPA
Pa.denititrificans  LAFYGAYVCLVLALVTYCMPLMKNR....DPYNQVLNMASFWLMSSGMVFMTVTLTPAGTVQTHLQRVEG
Pa.halodenitrificans LAFYGAYVMLLLGIISFAMPQLRRV....QPYNQVINMWGFWIMTGAMAFMTFTLTFAGVVQTHLQRVLG

                       420       430       440       450       460       470
Ps.nautica          SGEALSFMAGQDQIALFYWMRFVACAFFMACLVVYFGSFFIKGEASPAEEVRGPATADA.....
Ps.stutzeri         DGAAMSFMNTADQLAIFFWLRFIAGVFFLIGLVCYLYSFRQRGRVPVVVAAPAAA.........
Ps.aeruginosa       DGAAMTFMATQDQLAIFYWLREGACVVFLIGLVAYLLSFR.RGKAAA................
Pa.denititrificans  ....GFFMDVQDGLALFYWMRFGSCVAVVLGALLFIYAVLFPRREVVKAGPVQAHKDGHLEAAE
Pa.halodenitrificans ....MNFMEVQDQLVLFYGMRLASGVAVGIGACLLLYAFFGPAREQVPAGGTQLTSGTNRA...
```

Figure 1. Amino acid sequence comparison of the small (A) and large (B) subunits of *Ps. nautica* cNOR with other cNORs isolated from other bacteria.
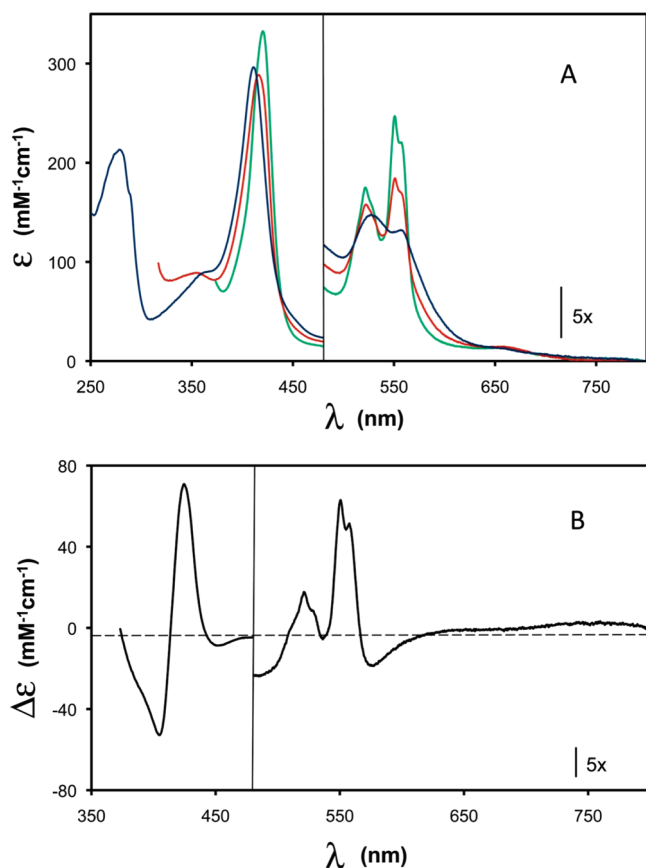
Figure 2. (A) UV/vis spectra of *Ps. nautica* cNOR in 100 mM pH 7 KPB, 0.02% dodecyl maltoside, 0.01% PE (as-isolated, blue line; ascorbate-reduced, red line; dithionite-reduced, green line). (B) Difference spectrum between the ascorbate-reduced spectrum and the dithionite-reduced spectrum (green minus red).

UV/vis Absorption Spectra. The as-purified *Ps. nautica* cNOR, at pH 7, displays a UV/vis spectrum (Figure 2A, blue line) typical of heme-containing proteins and very similar to those of other purified cNORs. The spectrum shows a protein peak at 280 nm, a Soret band at 411 nm, and a broad band at around 550 nm with two small absorption peaks at 530 and 560 nm in the β and α regions, respectively. The appearance of the small absorption peaks indicates the presence of a small amount of reduced heme, in accord with the Mössbauer data presented below. The absorbance ratio of the Soret band at 411 nm to the protein peak at 280 nm was determined to be 1.4. Protein determinations by both Lowry and BCA methods revealed interference from detergent present in the buffer. Thus, protein quantifications derived from amino acid composition were used to estimate an extinction coefficient of 295 mM^{-1} cm^{-1} at 411 nm for the oxidized cNOR. This value was then used to estimate protein concentration in all assays. It is important to note that while cNORs isolated from *Pa. denitrificans* and *H. halodenitrificans* exhibit an absorption band around 595 nm,[19,42] such a band is absent from the *Ps. nautica* cNOR. On the basis of a resonance Raman investigation, which suggests the presence of a μ-oxo group bridging heme b_3 and Fe$_B$ in the oxidized cNOR,[22] the 595 nm band has been attributed to a ligand-to-metal charge transfer band associated with a high-spin ferric heme b_3 without the proximal His ligand.[43] The absence of a 595 nm band in the as-purified *Ps. nautica* cNOR therefore suggests a different spin

state and/or a different coordination environment for heme b_3 (see below). A low-intensity broad band at around 662 nm is observed but shows no redox dependence, indicating minor presence of inactive protein.

Reducing the enzyme with ascorbate red-shifts the maximum of the Soret band to 418 nm and sharpens the optical bands in the α/β absorption region with maxima at 524 and 552 nm and a shoulder at 558 nm (Figure 2A, red line), consistent with reduction of low-spin heme groups. The absorption band at 552 nm has been assigned to heme c and the shoulder at 558 nm to heme b.[11,42,44] Thus, the optical data indicate both heme b and heme c are reduced by ascorbate. Upon reduction with sodium dithionite, the Soret maximum is further shifted to 422 nm and the α and β bands become more intense, indicating reduction of more heme groups (Figure 2A, green line). Figure 2B displays a difference spectrum (black line) between that of the dithionite- and ascorbate-reduced enzyme. On the basis of the following Mössbauer data, which indicate that only heme b_3 is oxidized in the ascorbate-reduced enzyme and that it can be reduced by dithionite, this difference spectrum represents absorption changes arising from the reduction of heme b_3 and indicates clearly that the reduced heme b_3 is low-spin. Reoxidation of the ascorbate- or dithionite-reduced enzyme produces a spectrum identical to that of the as-isolated enzyme, indicating reversible oxidation−reduction processes. In the presence of PMS, ascorbate can reduce the enzyme to a redox state equivalent to that of the dithionite-reduced cNOR as judged by optical spectroscopy (Figure S2).

Optical Oxidation/Reduction Titrations. The UV/vis spectrum of the as-purified *Ps. nautica* cNOR showed no pH dependence in the range of pH 5−9. To determine the redox properties of the metallocofactors, redox potentiometric titrations monitored by optical absorptions were performed at two pH values 6 and 7. The resulting spectra as a function of the redox potential at pH 7 (Figure 3A) were globally fitted (SPECFIT, Spectrum Software Associates) and spectral components deconvoluted. Good fits of the data were obtained by using two independent Nernst equations of different midpoint redox potentials that differ by ∼200 mV. At pH 7, the midpoint redox potentials were determined to be $E_I = +215 \pm 10$ mV and $E_{II} = -38 \pm 10$ mV, and at pH 6, $E_I = +232 \pm 10$ mV and $E_{II} = -16 \pm 10$ mV. To illustrate the goodness of our fits, in Figure 3B, we plotted the absorbance at 551 nm as a function of redox potential and compared the experimental data (circles) with the theoretical values (solid line) calculated by using the parameters obtained from the fits. On the basis of the Mössbauer and EPR data presented below, E_I is assigned to both heme c and heme b and E_{II} is assigned to heme b_3. As no absorption features are attributed to Fe$_B$, the redox potential of Fe$_B$ is not determined from this measurement. Optical redox titration has also been performed on *Pa. denitrificans* cNOR.[28] Although the midpoint potentials determined for the heme groups in *Pa. denitrificans* enzyme are about 100 mV higher than those reported here, the midpoint redox potentials for heme c (310 mV) and heme b (345 mV) in the *Pa. denitrificans* enzyme are also found to be comparable and are more than 200 mV above that of heme b_3 (60 mV). In other words, the large redox potential difference between the reactive heme b_3 and the electron-transfer heme groups, a functionally important factor, is conserved among cNOR's.

EPR Results. The as-purified *Ps. nautica* cNOR exhibits an EPR spectrum (Figure 4A) that is similar to those reported for
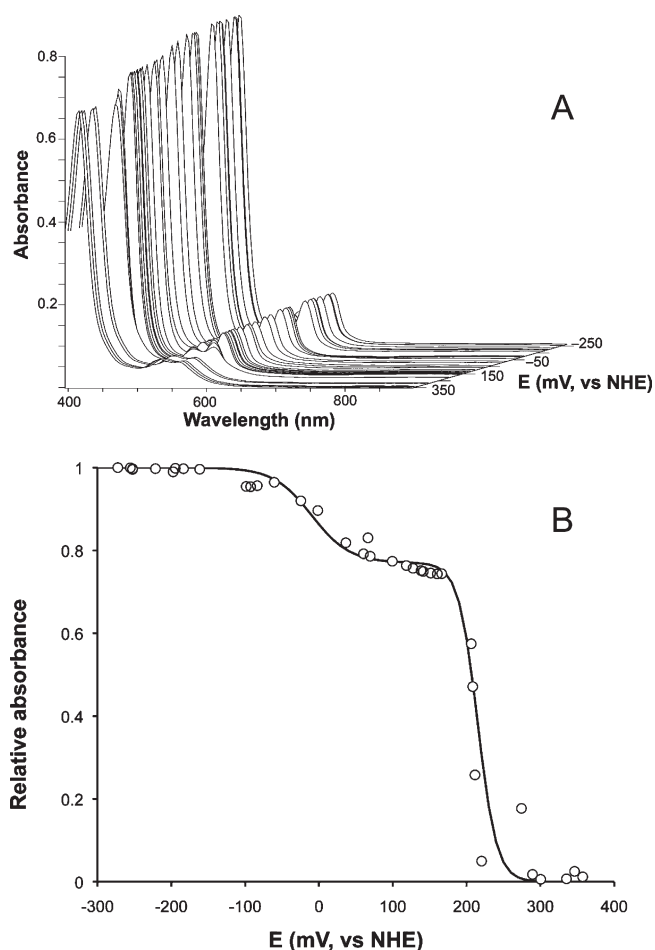
Figure 3. (A) UV/vis spectra of *Ps. nautica* cNOR as a function of redox potential at pH 7. (B) Absorbance at 551 nm as a function of redox potential at pH 7 (100 mM pH 7 KPB, 0.02% dodecyl maltoside, 0.01% PE). The solid line is the result calculated by using the parameters obtained from globally fitting the spectra shown in (A).

Figure 4. EPR spectra at 9.653 GHz of the as-isolated (A), ascorbate-reduced (B), and dithionite-reduced (C) *Ps. nautica* cNOR (265 μM in 100 mM KPB, pH 7, 0.02% DDM, 0.01% PE). Experimental conditions of spectra A−C: temperature = 12 K, microwave power = 0.2 mW, modulation frequency = 100 kHz, modulation amplitude = 0.5 mT, receiver gain = 1×10^5, conversion time = 163.84 ms, and time constant = 81.92 ms and of spectra D and E: microwave power = 6.3 mW, modulation frequency = 100 kHz, modulation amplitude = 0.4 mT, receiver gain = 2×10^5, conversion time = 81.92 ms, and time constant = 40.96 ms. Spectrum D was collected at 5.5 K, E at 7.0 K, F at 12 K, and G at 22.5 K.

other cNOR's.[19,21,42] Two sets of low-spin ferric heme signals are clearly visible. The prominent set of signals, with *g* values of 2.99, 2.26, and 1.43, have been attributed to the histidine−histidine ligated heme *b* of the NORB subunit.[21] The highly anisotropic set of signals, from which only the g_{max} value of 3.60 can be observed, have been attributed to the heme *c* of the NORC subunit.[45] Spin quantification of these two low-spin ferric heme signals were done using the Aasa and Vanngard method[46] modified according to De Vries and Albracht,[47] together with spectral simulation. Approximately 0.9 spin/molecule and 0.7 spin/molecule were determined for the heme *b* and heme *c* signals, respectively. (In our spin quantification estimations, $g_{mid} = 1.43$ and $g_{min} = 1.00$ were assumed for heme *c*.) In addition, a broad signal at *g* = 1.60, two derivative type signals at *g* = 2.01 and 2.05, and two overlapping signals at around *g* = 6.30 region are detected. The signals at *g* = 2.05 and 1.60, although not yet assigned, are present in other purified enzymes such as *Pa. denitrificans* and *Ps. aeruginosa* enzymes.[14,26] The current assumption is that in the oxidized enzyme the catalytic center is composed of a high-spin ferric heme b_3 antiferromagnetically coupled to a high-spin ferric Fe_B, resulting in a diamagnetic *S* = 0 ground state that yields no EPR resonances. The signals at the *g* = 6.30 region have been assigned to a small quantity of decoupled
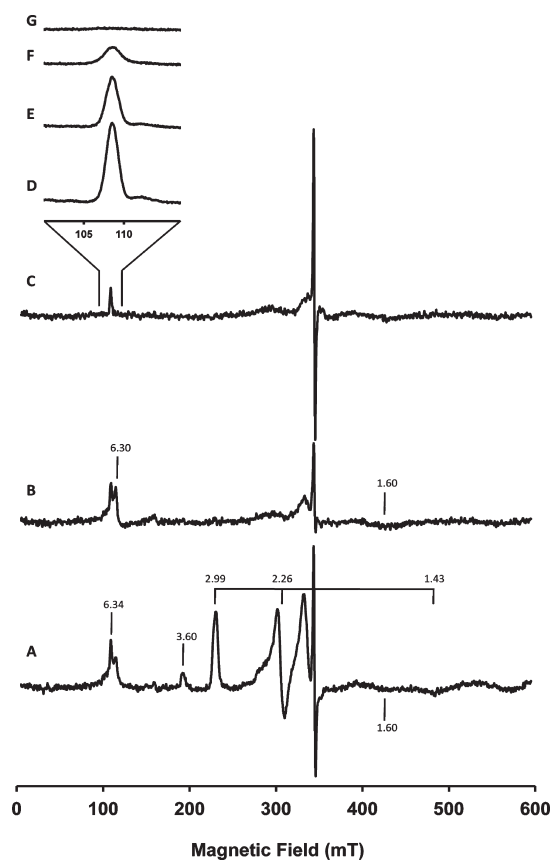
ferric high-spin heme b_3 and the signal at *g* = 2.01 to Fe_B or an organic radical.[19,42] The Mössbauer data, presented below, reveal that in the as-purified *Ps. nautica* NOR heme b_3 is in fact low-spin. Consequently, a re-evaluation of the above assignment for signals at the *g* = 6.3 region is required because a decoupled ferric low-spin heme b_3 would not produce signals at the *g* = 6 region.

Reduction of *Ps. nautica* cNOR with sodium ascorbate (1 mM) leads to the disappearance of the ferric low-spin signals (*g* = 3.60, 2.99, 2.26, and 1.45), while the signals around *g* = 6.30, 2.05, 2.01, and 1.60 are retained (Figure 4B). The disappearance of the ferric low-spin signals is consistent with the optical data (presented above) and the Mössbauer results (presented below), which show that heme *c* and heme *b* can be readily reduced by ascorbate to diamagnetic low-spin Fe^{II} states.

Further reduction with sodium dithionite eliminates the derivative-type EPR signal at the *g* = 6 region, but the sharp absorption-type signal at *g* = 6.34 is still clearly detectable (Figure 4C). Temperature dependence of this signal is characteristic of an electronic ground state system (Figure 4D−G). The Mössbauer data (presented below) show that in the ascorbate- and dithionite-reduced enzyme significant portions of Fe_B and
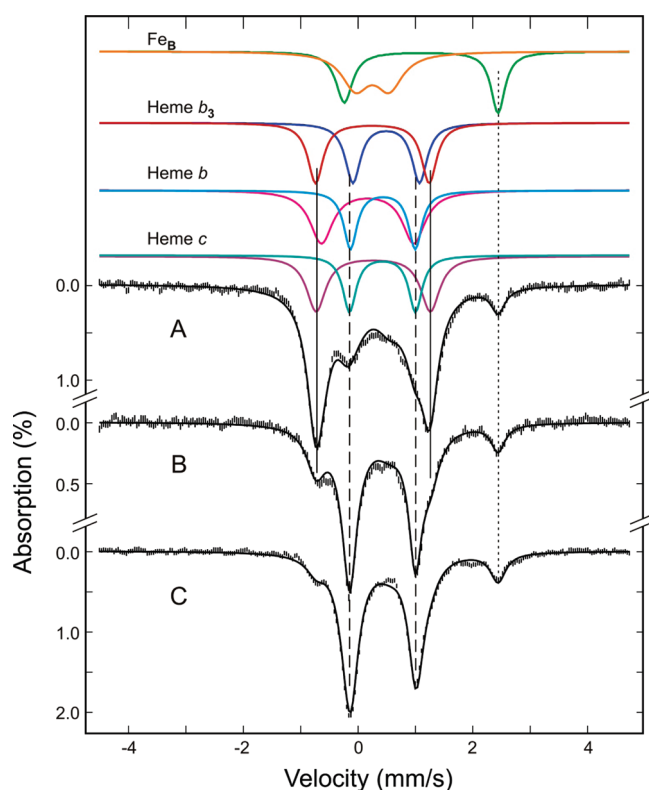
Figure 5. Mössbauer spectra of the as-purified (A), ascorbate-reduced (B), and dithionite-reduced (C) *Ps. nautica* cNOR (805 μM in 100 mM KPB, pH 7, 0.02% DDM, 0.01% PE). The spectra (vertical bars) were collected at 180 K in a weak magnetic field of 50 mT. The color lines displayed above the data are the deconvoluded spectra for the for Fe cofactors in the enzyme: Fe_B^{III}, orange; Fe_B^{II}, green; Fe^{III}-heme b_3, red; Fe^{II}-heme b_3, blue; Fe^{III}-heme b, magenta; Fe^{II}-heme b, cyan; Fe^{III}-heme c, purple; Fe^{II}-heme c, blue-green. The back solid lines overlaid with the experimental spectra are composite spectra simulated with the parameters and percent absorptions listed in Table 1. The dotted vertical line indicates the position of the high-energy line of the Fe_B^{II} doublet. The two solid vertical lines and the two dashed vertical lines respectively mark the general line positions of the doublets arising from the low-spin Fe^{II}-heme and Fe^{III}-heme cofactors.

heme b_3 remain in their oxidized states. It is therefore possible that the $g = 6.34$ signal could be associated with the oxidized heme b_3-Fe_B center.

Mössbauer Characterization. Mössbauer spectroscopy was used to further characterize the electronic states of the Fe centers and to provide direct and quantitative measurements on the compositions of the oxidation states of the Fe centers in various redox forms of the enzyme. Figure 5 shows the Mössbauer spectra of the as-purified (A), ascorbate-reduced (B), and dithionite-reduced (C) samples recorded at 180 K in a 50 mT magnetic field applied parallel to the γ-radiation. At this temperature, the electronic relaxation of Fe centers in proteins are generally fast in comparison with the ^{57}Fe nuclear precession, causing cancellation of the internal magnetic field at the ^{57}Fe nucleus and resulting in quadrupole doublets for the Fe centers. Thus, these spectra are composed of only quadrupole doublets arising from different Fe species, facilitating the analysis of the spectra. On the other hand, there are eight possible redox states for the four Fe sites in cNOR. Consequently, analysis of these spectra remains challenging, and a global analysis including all three spectra is applied.

First, the absorption peak at ~2.5 mm/s (indicated by a dotted line) can be assigned to the high-energy line of the quadrupole doublet arising from the high-spin ferrous Fe_B. Since this peak is well resolved from the rest of the absorptions, it allows for a reliable quantification on the amount of reduced Fe_B in the sample. It is therefore interesting to note that all three forms of the enzyme contain detectable amounts of reduced Fe_B, including the as-purified sample. Second, the most prominent feature observed in the spectrum of the as-purified sample (Figure 5A) is a broad quadrupole doublet (line positions indicated by two vertical lines) with apparent parameters ($\Delta E_Q \sim 2$ mm/s and $\delta \sim 0.2$ mm/s) that are indicative of $S = 1/2$ low-spin ferric heme species. A rough estimate of its absorption area indicates that this doublet accounts for ~70% of the total Fe in the sample. Since heme b and heme c can contribute up to a maximum of only 50%, the remaining contribution has to arise from heme b_3. In other words, *the oxidized heme b_3 in Ps. nautica cNOR is a low-spin ferric heme*, in contrast to the high-spin ferric states reported for heme b_3 of cNOR's from other organisms.[42,43] Upon addition of sodium ascorbate, the intensity of this low-spin ferric—heme doublet decreases to about 25% of the total Fe absorption, and a new doublet (indicated by two vertical dashed lines), accounting for ~50% of the Fe absorption, is detected (Figure 5B). The apparent parameters for this doublet ($\Delta E_Q \sim 1.1$ mm/s and $\delta \sim 0.4$ mm/s) are characteristics for low-spin ferrous hemes. Taking into consideration the midpoint redox potentials determined for the three heme groups (see above), only the electron-transfer heme c and heme b are reducible by ascorbate. Thus, this new doublet is assigned to the reduced heme b and heme c. With this assignment, it becomes obvious that in the spectrum of the as-purified enzyme (Figure 5A) there are absorptions arising from these reduced hemes. In other words, heme b and heme c are partially reduced in the as-purified enzyme, in agreement with the optical data described above. Observation of partial reduction of heme b and heme c in the as-purified enzyme is consistent with the high midpoint redox potential (215—230 mV) determined for these heme groups. Addition of sodium dithionite further decreases the intensity of the low-spin ferric heme doublet and increases the intensity of the low-spin ferrous heme doublet (Figure 5C), indicating that the active site heme b_3 is partially reduced by dithionite and that the reduced heme b_3 is also low-spin.

With the above understanding, it is possible to analyze these three spectra simultaneously using one set of parameters. To reduce the number of variable parameters, the following rational assumptions were made: (1) the total absorption intensity (oxidized plus reduced) for each one of the four Fe sites is 1/4 of the total Fe absorption, (2) the line widths of a quadrupole doublet arising from a heme group are the same, and (3) for each sample, the [oxidized]/[reduced] ratio of heme b and heme c is the same. (This assumption is based on the observed similar midpoint redox potentials for heme b and heme c; see above.) During the analysis, we also realized that the electronic relaxation rate of ferric Fe_B is not much faster than the ^{57}Fe precession rate, resulting in a broad and featureless spectrum. A broad quadrupole doublet was therefore used to approximate the spectrum of ferric Fe_B. The results of the least-squares fit are presented in Figure 5 and Table 1. The parameters obtained are consistent with high-spin states for the oxidized and reduced Fe_B, as expected for most non-heme Fe cofactors in proteins, and low-spin states for all three heme groups regardless of their redox states, suggesting 6-coordinate environments for both ferric and

Table 1. Mössbauer Parameters and Percent Absorptions of Fe Cofactors in the As-Purified, Ascorbate-Reduced, and Dithionite-Reduced cNOR from *Ps. nautica*[a]

cofactor	δ (mm/s)	ΔE_Q (mm/s)	absorption (%)		
			as-purified	ascorbate-reduced	dithionite-reduced
Fe_B^{II}	1.10	2.68	8 (1)	11 (1)	15 (2)
Fe_B^{III}	0.25	0.59	17 (2)	14 (2)	10 (1)
Fe^{II}-heme b_3	0.49	1.17	0	0	15 (2)
Fe^{III}-heme b_3	0.25	1.99	25 (3)	25 (3)	10 (1)
Fe^{II}-heme b	0.43	1.13	3 (1)	25 (3)	25 (3)
Fe^{III}-heme b	0.23	2.04	22 (2)	0	0
Fe^{II}-heme c	0.43	1.15	3 (1)	25 (3)	25 (3)
Fe^{III}-heme c	0.17	1.61	22 (2)	0	0

[a] The values in parentheses give the uncertainties in the last significant digits estimated for the percent absorptions. Because of the complexity of the spectra, the Mössbauer parameters (δ and ΔE_Q) were fixed during the least-squares fittings. The line widths of the quadrupole doublets used in our fits are 0.28 mm/s for Fe^{II}-heme b and Fe^{II}-heme c, 0.4 mm/s (left line) and 0.3 mm/s (right line) for Fe^{III}-heme b, 0.3 mm/s (left) and 0.5 mm/s (right) for Fe^{III}-heme c, 0.28 mm/s (left) and 0.35 mm/s (right) for Fe^{II}-heme b_3, 0.36 mm/s (left) and 0.43 mm/s (right) for Fe^{III}-heme b_3, 0.35 mm/s (left) and 0.3 mm/s (right) for Fe_B^{II}.

Table 2. Specific Activity of *Ps. nautica* cNOR as a Function of Electron Donor and Assay Conditions[a]

electron donor	specific activity (μmol min^{-1} mg^{-1})
none	
ascorbate + PMS + oxidized horse heart cyt. c	3.8
ascorbate + PMS	4.3
PMS + reduced horse heart cyt. c	0.7
ascorbate	0.7
PMS	<0.1
reduced horse heart cyt. c	<0.1
reduced *Ps. nautica* cyt. c_{552}	3.5
reduced *Ps. nautica* cyt. c_{552}	0.6[b]
reduced *Ps. nautica* cyt. c_{549}	<0.1[b]
reduced *Ps. nautica* cyt. c_{551}	<0.1[b]
reduced *Ps. nautica* cyt. c_{553}	<0.1[b]
reduced *Ps. nautica* cyt. $c_{553(548)}$	<0.1[b]
reduced *Ps. nautica* cyt. c_4	<0.1[b]

[a] Errors between duplicates are approximately ±20%. Concentrations used in the assay solutions are [cNOR] = 70 nM, [ascorbate] = 10 mM, [PMS] = 100 μM, and [cyt.] = 20 μM. [b] [cyt.] = 3 μM in the assay solution (see text).

ferrous hemes. The Mössbauer percent absorptions determined for the quadrupole doublets (Table 1) provide a quantitative assessment of the redox status of all four Fe cofactors in the three different oxidation states of the enzyme: heme b and heme c are partially reduced (3/25 = 12%) in the as-purified enzymes and can be completely reduced by ascorbate. Heme b_3 is fully oxidized in the as-purified enzyme and cannot be reduced by ascorbate alone. This observation is consistent with the 200 mV redox potential difference detected between heme b_3 and the two electron transfer heme b and heme c. In the as-purified enzyme, Fe_B is significantly reduced ($\sim$30% reduction), and yet in the dithionite-reduced enzyme, it is only partially reduced. The level of reduction (60%), interestingly, is identical to that of heme b_3, suggesting the presence of interactions between Fe_B and heme b_3 which could complicate their redox behaviors. The Mössbauer

results, taken together with results obtained from enzymatic activity studies (presented below), provide information for determining the "active" redox-state of the enzyme, information that is essential for understanding enzyme mechanism.

Enzymatic Activities. As a reference, specific activity of the as-purified enzyme (Table 2) was first determined by using the established assay developed by Girsh et al.,[19] in which the assay solution contains 10 mM sodium ascorbate, 100 μM PMS, and 20 μM horse heart cytochrome c in 20 mM KPB at pH 6. The specific activity values obtained are comparable to reported values for *Pa. denitrificans* and *Ps. aeruginosa* enzymes at this pH.[28,51]

Examinations on the effects of various electron donors revealed that horse heart cytochrome c had no effect on the enzymatic activity and was ineffective as an electron donor. Presence of ascorbate and PMS in the assay solution was sufficient to produce full activity of the enzyme. Interestingly, *Ps. nautica* cytochrome c_{552} was found to be an effective electron donor and could produce fully active enzymes (Table 2). In an effort to obtain further evidence to support c_{552} as the physiological electron donor for *Ps. nautica* cNOR, a set of enzymatic assays was performed with six different low-spin cytochromes obtained from *Ps. nautica* (cytochromes c_{551}, c_{552}, c_{459}, c_{553}, $c_{553(548)}$ and membrane bound cytochrome c_4).[31,32,48] In this series of experiments, due to limits in the amounts of some of the purified cytochromes, the experiments were carried out with 3 μM of cytochromes. Only the periplasmatic cythocrome c_{552} was found to show a significant value of specific activity. All other cytochromes were ineffective in providing electrons to *Ps. nautica* cNOR (last six rows, Table 2).

It is interesting to note that the midpoint redox potential of *Ps. nautica* c_{552} is about +250 mV at pH 7.6,[32] which is more than 200 mV higher than the reduction potential for heme b_3. From a purely thermodynamical consideration, this suggests that c_{552} may not be a good electron donor for cNOR. But, as presented above, we have shown that c_{552} is the only small cytochrome that is capable to catalyze the reduction of NO. In fact, the same concern can also be raised for heme c and heme b because their midpoint redox potentials are also much higher than that of heme b_3. Taking these observations into consideration, we suggest that the initial reductive activation of heme b_3 and the transfer of electrons from cytochrome c_{552}, heme b, and heme c to the diiron

active site for NO reduction are separate events that could have distinct electron transfer pathways.

■ DISCUSSION

Spin State of Heme b_3. We have purified *Ps. nautica* cNOR to homogeneity and characterized the purified enzyme in detail by using biochemical and spectroscopic methods. The purified enzyme exhibits an optical spectrum with an absorbance ratio of $A_{411}/A_{280} = 1.4$, one of the highest purity preparations ever reported for cNOR. Heme and Fe content determinations show a cofactor stoichiometry of 1:2:1 for heme *c*:heme *b*:non-heme iron per molecule of cNOR, indicating full occupancy of metal centers in the purified enzyme. Regarding metal content, *Ps. nautica* cNOR was found to contain Ca. While the value obtained is substoichiometric, the presence of calcium was also observed in the X-ray crystallographic structure of the *Ps. aeruginosa* enzyme,[51] indicating that Ca presence might be a common feature between anaerobic and microaerobic respiratory enzymes. As shown in Figure 1, arginine residues 50 and 433 (*Ps. nautica* numbering) are conserved in the five *Pseudomonas* and *Paracoccus* sequences. These residues are also present in Ca binding in cbb_3 cytochrome oxidase from *Ps. stutzeri*.[59]

Consistent with results reported for cNORs isolated from other organisms, the spectroscopic data indicate that the spin states of the electron transfer heme *c* and heme *b* are low-spin, and for the non-heme iron Fe$_B$, it is high-spin. Contrary to the conventionally assumed high-spin state for heme b_3, the Mössbauer data revealed that the spin state of the catalytic heme b_3 is in fact low-spin. The UV/vis difference spectrum between the spectra of ascorbate-reduced and dithionite-reduced enzyme (Figure 2B), which displays the difference arising from changes in the oxidation state of heme b_3, supports the low-spin designation and indicates further that at room temperature the reduced heme b_3 remains low-spin. In support of our finding, a recent X-ray crystallographic structure of the *Ps. aeruginosa* enzyme, published online by Hino and co-workers[51] while this manuscript was in the reviewing process, shows that heme b_3 is indeed hexacoordinated. It is axialy coordinated to a His residue (H347, *Ps. stutzeri* numbering) and a μ-oxo (or a possible μ-hydroxo) bridge to Fe$_B$. On the basis of temperature-dependent MCD and low-temperature EPR data, Cheesman et al.[21] concluded that the spin state of heme b_3 in oxidized *Ps. stutzeri* cNOR underwent a spin transition from high spin at room temperature to low spin at 4.2 K. Our spectroscopic analysis clearly shows that heme b_3 is low-spin in the ferric state between 4.2 and 180 K and in the ferrous active form from 4.2 K up to room temperature.

Reconsideration of the g = 6.34 Assignment. In the oxidized enzyme, the ferric heme b_3 is bridging to the ferric Fe$_B$ via an oxo group.[22,51] Prior to this investigation, heme b_3 was assumed to be high-spin ferric[42,45] antiferromagnetically coupled to the ferric high-spin ($S = 5/2$) Fe$_B$, forming a diamagnetic ($S = 0$) ground state. Thus, no EPR signal was expected to arise from the oxidized catalytic diiron center. The signals at the g = 6 region were then assigned to a small quantity of uncoupled heme b_3. Also, previously, a g = 4.3 signal was detected and had been assigned to a minor quantity of the uncoupled ferric Fe$_B$. For the as-purified *Ps. nautica* cNOR, however, this g = 4.3 signal is almost nonobservable (Figure 4A). We therefore proposed that the previously detected g = 4.3 signal may not arise from an uncoupled Fe$_B$ but, rather, represent minor adventitiously bound ferric

impurity, which is not present in our as-purified *Ps. nautica* cNOR.

Here, we present spectroscopic data establishing unambiguously that heme b_3 is low-spin at low temperature (4.2−180 K). Spin−spin coupling of a low-spin ferric ($S = 1/2$) heme b_3 with a high-spin ferric ($S = 5/2$) Fe$_B$ would yield an integer-spin ground state with $S = 2$ or $S = 3$ that may not be EPR silent.[49] On the basis of the following observations, we propose that the g = 6.34 signal may arise from the oxidized binuclear heme b_3-Fe$_B$ site. (1) The absorption-type signal detected at g = 6.34 for cNORs is distinct from the derivative-type g = 6 signal expected for a high-spin ferric heme (Figure 4D−G). (2) In the as-purified enzyme, there are four Fe cofactors that could be detected by EPR. The electron-transfer ferric low-spin heme *c* and heme *b* are completely accounted for by the two sets of low-spin ferric EPR signals. Thus, the g = 6.34 signal has to be arising from either heme b_3 or Fe$_B$ or both. Because an isolated low-spin ferric heme b_3 cannot yield signals at the g = 6 region and because no additional signals are detected that may be assigned to an isolated low-spin ferric heme b_3 or to an isolated ferric high-spin Fe$_B$, a probable explanation would be that heme b_3 and Fe$_B$ are spin coupled to form an integer-spin system that yields the g = 6.34 signal. And, (3) the g = 6.34 signal is detected in all three oxidation states of the enzyme (as purified, ascorbate-reduced, and ditionite-reduced). According to the Mössbauer data (Table 1), the only common oxidation state for all the Fe cofactors that is present in all three oxidation states of the enzyme and may be detectable by EPR is the Fe^{III}−heme b_3−Fe$_B^{III}$ site. Taken together, these observations argue favorably for the g = 6.34 signal to arise from a spin-coupled oxidized heme b_3−Fe$_B$ center. A definitive assignment for the g = 6.34 signal and a complete understanding of the nature of the proposed heme b_3−Fe$_B$ spin−spin coupling, however, will require further detailed spectroscopic investigations, such as parallel mode EPR studies coupled with low-temperature-high-field Mössbauer measurements. Finally, it is important to point out that the g = 6.34 signal have been observed for all as-purified cNORs that have been characterized by EPR. Consequently, if the g = 6.34 signal is indeed arising from a spin-coupled binuclear center comprising a low-spin ferric heme b_3 and a high-spin ferric Fe$_B$, then heme b_3 is most likely low-spin in all cNORs in the experimental conditions studied.

Catalytic Site Coordination. In general, high-spin heme complexes are five-coordinated, while low-spin heme complexes are six-coordinated, except for the low-spin [FeNO]^7 heme complexes, which can be either five- or six-coordinated. The fact that heme b_3 is low-spin in both its oxidized and reduced states implies that it is six-coordinated, rather than five-coordinated as previously assumed. On the basis of amino acid sequence analysis and spectroscopic data comparison, we believe that H340 (*Ps. nautica* numbering) and a μ-oxo bridge to Fe$_B$ (for ferric heme b_3 states) or a hydroxide anion (in the fully reduced enzyme) are responsible for the observed low-spin state of heme b_3. The presence of a sixth ligand for heme b_3 is consistent with fast kinetic measurements for CO binding,[60] where it was found that the initial binding of CO to Fe^{II}−heme b_3 is ∼3 orders of magnitude slower than photolysis-induced CO recombination, presumably reflecting the need to displace a blocking axial ligand. By comparison with the known ligands of Fe$_B$ in *Ps. aeruginosa* NOR, we attribute residues H200, H251, H252, and E204 as ligands to the non-heme iron.

Redox State of the Active Enzyme. An important information that is absolutely required for understanding enzyme mechanism is the redox state of the active enzyme. For cNOR, both the three-electron reduced state (heme b, heme c, and Fe_B are reduced while heme b_3 is oxidized)[28] and the fully reduced state[14,19,50] have been proposed to be the active redox state. By exploiting the large midpoint redox potential differences between heme b_3 and the electron transfer heme c and heme b, we attempted to address this important question by preparing a stable three-electron-reduced enzyme for activity assay. We reduced the as-purified enzyme by using a mild reductant, ascorbate, and characterized the oxidation states of the cofactors by using Mössbauer spectroscopy. The results show that heme b and heme c are completely reduced while heme b_3 remains oxidized (Table 1). Approximately half of Fe_B is reduced. Activity assay indicates that the ascorbate-reduced cNOR is inactive (Table 2). The PMS and ascorbate (that have been used by several authors to reduce the enzyme in the activity assay) has been proved by UV/vis spectroscopy to yield a redox state similar to the one achieved by dithionite reduction (Figure S2). We therefore conclude that heme b_3 has to be reduced for the enzyme to be active and that the fully reduced state is likely the active state of the enzyme.

Mechanistic Consideration. Currently, there are two proposed mechanisms for NO reduction by cNOR: the *cis*- and *trans*-mechanism (see Introduction). A major distinction between these two mechanisms is at the initial step of coordinating two NO molecules at the binuclear center. In the *cis*-mechanism, both NO molecules are coordinated either to the reduced Fe_B or to heme b_3 forming a Fe^{II}—dinitrosyl complex.[28] In the *trans*-mechanism, one NO molecule is bound to each reduced Fe site of the binuclear center forming a $[FeNO]_2^7$ complex.[14] The *cis*-mechanism with two NO molecules bound to a reduced heme b_3 has been questioned based on the fact that these types of complexes are too stable for turnover.

To prevent the binding of NO to a Fe^{II}—heme b_3 forming a stable $[FeNO]^7$—heme complex in the initial NO binding step, it has been proposed that the three-electron reduced state with an oxidized heme b_3 is the active state of the enzyme.[28] Our conclusions that the fully reduced state is the active form of the enzyme and that heme b_3 is six-coordinated suggest an alternative possibility that favors NO binding to Fe_B in the initial catalytic step: The presence of a sixth ligand weakens the affinity of NO binding to heme b_3 and promotes the formation of a Fe^{II}—dinitrosyl complex at Fe_B. In such a scenario, the initial function of heme b_3 could be (1) to assist in adjusting the orientation of the Fe_B-bound NO molecules and subsequent formation of the N—N bond and (2) to provide the essential electron for the reduction of NO. Without further kinetic data, we cannot exclude that at a later mechanistic step heme b_3 will somehow bind to NO (or to a reaction intermediate). Recently, Lachmann and co-workers[52] demonstrated that CO binds to reduced heme b_3 (probably displacing the sixth ligand initially present) and that flash-induced dissociation causes heme b_3 oxidation and catalysis. It is also known that for the CO-bound enzyme NO can still bind to the Fe_B site.[14] Both observations support the possibility of an initial binding of NO to Fe_B. It is important to comment that we believe that the *cis*-mechanism (with ligation of NO to Fe_B) is energetically favorable. The NO dissociation rate constants for reduced b-type ferrous porphyrin complexes are in the order of 10^{-3}—10^{-5} s^{-1}, demonstrating the stability of this type of nitrosyl complex.[53−56] To our knowledge

very few hemic proteins form unstable/transient nitrosyl complexes: NO synthase, cytochrome cd_1-type nitrite reductase, and cytochrome P450 all exhibit fast NO dissociation rate constants $(2-100$ s$^{-1})$. One should mention that even with NO synthase, an enzyme that catalyzes the formation of NO, the release of NO is only productive from a Fe^{III}—heme—NO catalytic intermediate and very slow from the reduced Fe^{II}—heme—NO form.[57] In the case of cytochrome cd_1 nitrite reductase from denitrifying bacteria the fast NO dissociation from the ferrous heme form is thought to be associated with the involvement of heme d_1. Fungal NOR, a member of the cytochrome P450 family, contains a heme b with axial cysteinate coordination. The NO substrate binds to the ferric state of heme b, leading to the formation of a 6-coordinated ferric—heme—nitrosyl first intermediate. The Fe^{III}—NO complex is unstable, and the dissociation of NO is due to the presence of the cysteinyl ligand and to the ferric state of the heme, such as in NO synthase.

It is worth noting that *Ps. nautica* NOR is also able to reduce molecular oxygen.[58] Although it is not established how widespread such bifunctionality is among cNOR, the fact that it was not reported for all characterized enzymes might be an indication that an alternative mechanism cannot be excluded.

■ ASSOCIATED CONTENT

Ⓢ Supporting Information. Figure S1 showing the DNA and deduced amino acid sequence of *Ps. nautica* NOR and Figure S2 comparing the UV/vis spectrum of dithionite-reduced cNOR with that of the enzyme reduced by ascorbate plus PMS. This material is available free of charge via the Internet at http://pubs.acs.org.

■ AUTHOR INFORMATION

Corresponding Author
*E-mail: alice.pereira@dq.fct.unl.pt (A.S.P.), isa@dq.fct.unl.pt (I.M.). Phone: 351-212948345. Fax: 351-212948550.

■ ACKNOWLEDGMENT

■ ABBREVIATIONS

NOR, nitric oxide reductase; EPR, electron paramagnetic resonance; PMSF, phenylmethylsulfonyl fluoride; DDM, sodium n-dodecyl α-D-maltoside; DEAE, diethylaminoethyl cellulose; SDS-PAGE, sodium dodecyl sulfate polyacrylamide gel electrophoresis; BCA, bicinchoninic acid; TPTZ, 2,4,6-tripyridyl-s-triazine; CTAB, cetyltrimethylammonium bromide; PMS, phenazine methosulfate; PE, 2-phenylethanol.

■ REFERENCES

(1) Bonin, P., Bertrand, J. C., Giordano, G., and Gilewicz, M. (1987) Specific sodium dependence of a nitrate reductase in a marine bacterium. *FEMS Microbiol. Lett. 48*, 5–9.

(2) Bonin, P., Gilewicz, M., Denis, M., and Bertrand, J. C. (1989) Salt requirements in the denitrifying bacterium *Pseudomonas nautica* 617. *Res. Microbiol. 140*, 159–169.

(3) Tavares, P., Pereira, A. S., Moura, J. J., and Moura, I. (2006) Metalloenzymes of the denitrification pathway. *J. Inorg. Biochem. 100* 2087–2100.

(4) Brown, K., Djinovic-Carugo, K., Haltia, T., Cabrito, I., Saraste, M., Moura, J. J., Moura, I, Tegoni, M., and Cambillau, C. (2000) Revisiting the catalytic CuZ cluster of nitrous oxide (N_2O) reductase. Evidence of a bridging inorganic sulfur. *J. Biol. Chem. 275*, 41133–41136.

(5) Lopes, H., Besson, S., Moura, I., and Moura, J. J. (2001) Kinetics of inter- and intramolecular electron transfer of *Pseudomonas nautica* cytochrome cd_1 nitrite reductase: regulation of the NO-bound end product. *J. Biol. Inorg. Chem. 6*, 55–62.

(6) Brown, K., Tegoni, M., Prudencio, M., Pereira, A. S., Besson, S., Moura, J. J., Moura, I., and Cambillau, C. (2000) A novel type of catalytic copper cluster in nitrous oxide reductase. *Nat. Struct. Biol. 7*, 191–195.

(7) Correia, C., Besson, S., Brondino, C. D., Gonzalez, P. J., Fauque, G., Lampreia, J., Moura, I., and Moura, J. J. (2008) Biochemical and spectroscopic characterization of the membrane-bound nitrate reductase from *Marinobacter hydrocarbonoclasticus* 617. *J. Biol. Inorg. Chem. 13*, 1321–1333.

(8) Heiss, B., Frunzke, K., and Zumft, W. G. (1989) Formation of the N-N bond from nitric oxide by a membrane-bound cytochrome *bc* complex of nitrate-respiring (denitrifying) *Pseudomonas stutzeri. J. Bacteriol. 171*, 3288–3297.

(9) Kastrau, D. H., Heiss, B., Kroneck, P. M., and Zumft, W. G. (1994) Nitric oxide reductase from *Pseudomonas stutzeri*, a novel cytochrome *bc* complex. Phospholipid requirement, electron paramagnetic resonance and redox properties. *Eur. J. Biochem. 222*, 293–303.

(10) Hoglen, J., and Hollocher, T. C. (1989) Purification and some characteristics of nitric oxide reductase-containing vesicles from *Paracoccus denitrificans. J. Biol. Chem. 264*, 7556–7563.

(11) Carr, G. J., and Ferguson, S. J. (1990) The nitric oxide reductase of *Paracoccus denitrificans. Biochem. J. 269*, 423–429.

(12) Sakurai, T., Nakashima, S., Kataoka, K., Seo, D., and Sakurai, N. (2005) Diverse NO reduction by *Halomonas halodenitrificans* nitric oxide reductase. *Biochem. Biophys. Res. Commun. 333*, 483–487.

(13) Sakurai, T., Sakurai, N., Matsumoto, H., Hirota, S., and Yamauchi, O. (1998) Roles of four iron centers in *Paracoccus halodenitrificans* nitric oxide reductase. *Biochem. Biophys. Res. Commun. 251*, 248–251.

(14) Kumita, H., Matsuura, K., Hino, T., Takahashi, S., Hori, H., Fukumori, Y., Morishima, I., and Shiro, Y. (2004) NO reduction by nitric-oxide reductase from denitrifying bacterium *Pseudomonas aeruginosa*: characterization of reaction intermediates that appear in the single turnover cycle. *J. Biol. Chem. 279*, 55247–55254.

(15) Cramm, R., Pohlmann, A., and Friedrich, B. (1999) Purification and characterization of the single-component nitric oxide reductase from *Ralstonia eutropha* H16. *FEBS Lett. 460*, 6–10.

(16) Hendriks, J., Oubrie, A., Castresana, J., Urbani, A., Gemeinhardt, S., and Saraste, M. (2000) Nitric oxide reductases in bacteria. *Biochim. Biophys. Acta 1459*, 266–273.

(17) Householder, T. C., Fozo, E. M., Cardinale, J. A., and Clark, V. L. (2000) Gonococcal nitric oxide reductase is encoded by a single gene, *norB*, which is required for anaerobic growth and is induced by nitric oxide. *Infect. Immun. (68)*, 5241–5246.

(18) Suharti, Heering, H. A., and de Vries, S. (2004) NO reductase from *Bacillus azotoformans* is a bifunctional enzyme accepting electrons from menaquinol and a specific endogenous membrane-bound cytochrome c_{551}. *Biochemistry 43*, 13487–13495.

(19) Girsch, P., and de Vries, S. (1997) Purification and initial kinetic and spectroscopic characterization of NO reductase from *Paracoccus denitrificans. Biochim. Biophys. Acta 1318*, 202–216.

(20) Hendriks, J., Warne, A., Gohlke, U., Haltia, T., Ludovici, C., Lubben, M., and Saraste, M. (1998) The active site of the bacterial nitric oxide reductase is a dinuclear iron center. *Biochemistry 37*, 13102–13109.

(21) Cheesman, M. R., Zumft, W. G., and Thomson, A. J. (1998) The MCD and EPR of the heme centers of nitric oxide reductase from *Pseudomonas stutzeri*: Evidence that the enzyme is structurally related to the heme-copper oxidases. *Biochemistry 37*, 3994–4000.

(22) Moenne-Loccoz, P., Richter, O. M. H., Huang, H. W., Wasser, I. M., Ghiladi, R. A., Karlin, K. D., and de Vries, S. (2000) Nitric oxide reductase from *Paracoccus denitrificans* contains an oxo-bridged heme/ non-heme diiron center. *J. Am. Chem. Soc. 122 (38)*, 9344–9345.

(23) Moenne-Loccoz, P. (2007) Spectroscopic characterization of heme iron-nitrosyl species and their role in NO reductase mechanisms in diiron proteins. *Nat. Prod. Rep. 24 (3)*, 610–620.

(24) Zumft, W. G. (2005) Nitric oxide reductases of prokaryotes with emphasis on the respiratory, heme-copper oxidase type. *J. Inorg. Biochem. 99*, 194–215.

(25) Watmough, N. J., Field, S. J., Hughes, R. J., and Richardson, D. J. (2009) The bacterial respiratory nitric oxide reductase. *Biochem. Soc. Trans. 37*, 392–399.

(26) Field, S. J., Thorndycroft, F. H., Matorin, A. D., Richardson, D. J., and Watmough, N. J. (2008) The respiratory nitric oxide reductase (NorBC) from *Paracoccus denitrificans. Methods Enzymol. 437*, 79–101.

(27) Collman, J. P., Dey, A., Yang, Y., Decreau, R. A., Ohta, T., and Solomon, E. I. (2008) Intermediates Involved in the Two Electron Reduction of NO to N(2)O by a Functional Synthetic Model of Heme Containing Bacterial NO Reductase. *J. Am. Chem. Soc. 130*, 16498–16499.

(28) Gronberg, K. L., Roldan, M. D., Prior, L., Butland, G., Cheesman, M. R., Richardson, D. J., Spiro, S., Thomson, A. J., and Watmough, N. J. (1999) A low-redox potential heme in the dinuclear center of bacterial nitric oxide reductase: implications for the evolution of energy-conserving heme-copper oxidases. *Biochemistry 38*, 13780–13786.

(29) Gronberg, K. L., Watmough, N. J., Thomson, A. J., Richardson, D. J., and Field, S. J. (2004) Redox-dependent open and closed forms of the active site of the bacterial respiratory nitric-oxide reductase revealed by cyanide binding studies. *J. Biol. Chem. 279*, 17120–17125.

(30) Schagger, H., and von Jagow, G. (1987) Tricine-sodium dodecyl sulfate-polyacrylamide gel electrophoresis for the separation of proteins in the range from 1 to 100 kDa. *Anal. Biochem. 166*, 368–379.

(31) Saraiva, L. M., Besson, S., Moura, I., and Fauque, G. (1995) Purification and preliminary characterization of three *c*-type cytochromes from *Pseudomonas nautica* strain 617. *Biochem. Biophys. Res. Commun. 212*, 1088–1097.

(32) Saraiva, L. M., Fauque, G., Besson, S., and Moura, I. (1994) Physico-chemical and spectroscopic properties of the monohemic cytochrome C_{552} from *Pseudomonas nautica* 617. *Eur. J. Biochem. 224*, 1011–1017.

(33) Lowry, O. H., Rosebrough, N. J., Farr, A. L., and Randall, R. J. (1951) Protein Measurement with the Folin Phenol Reagent. *J. Biol. Chem. 193*, 265–275.

(34) Berry, E. A., and Trumpower, B. L. (1987) Simultaneous determination of hemes *a*, *b*, and *c* from pyridine hemochrome spectra. *Anal. Biochem. 161*, 1–15.

(35) Fischer, D. S., and Price, D. C. (1964) A simple serum iron method using the new sensitive chromogen tripyridyl-S-triazine. *Clin. Chem. 10*, 21–31.

(36) Moore, S., and Stein, W. H. (1963) Chromatographic determination of amino acids by the use of automatic recording equipment. *Methods Enzymol. 6*, 819–831.

(37) Ausubel, F. M., Brent, R., Kingston, R. E., Seidman, J. G., Smith, J. A., and Struhl, K., (Eds.) (1989) *Current Protocols in Molecular Biology*, Greene Pub. Associates and Wiley-Interscience, New York.

(38) Butland, G., Spiro, S., Watmough, N. J., and Richardson, D. J. (2001) Two conserved glutamates in the bacterial nitric oxide reductase are essential for activity but not assembly of the enzyme. *J. Bacteriol. 183*, 189–199.

(39) Flock, U., Thorndycroft, F. H., Matorin, A. D., Richardson, D. J., Watmough, N. J., and Adelroth, P. (2008) Defining the proton

entry point in the bacterial respiratory nitric-oxide reductase. *J. Biol. Chem. 283*, 3839–3845.

(40) Thorndycroft, F. H., Butland, G., Richardson, D. J., and Watmough, N. J. (2007)A new assay for nitric oxide reductase reveals two conserved glutamate residues form the entrance to a proton-conducting channel in the bacterial enzyme. *Biochem. J. 401*, 111–119.

(41) Flock, U., Lachmann, P., Reimann, J., Watmough, N. J., and Ädelroth, P. (2009)Exploring the terminal region of the proton pathway in the bacterial nitric oxide reductiase. *J. Inorg. Biochem. 103*, 845–850.

(42) Sakurai, N., and Sakurai, T. (1997)Isolation and characterization of nitric oxide reductase from *Paracoccus halodenitrificans*. *Biochemistry 36*, 13809–13815.

(43) Field, S. J., Prior, L., Roldan, M. D., Cheesman, M. R., Thomson, A. J., Spiro, S., Butt, J. N., Watmought, N. J., and Richardson, D. J. (2002)Spectral properties of bacterial nitric-oxide reductase - Resolution of pH-dependent forms of the active site heme $b(3)$. *J. Biol. Chem. 277* (23), 20146–20150.

(44) Fujiwara, T., and Fukumori, Y. (1996)Cytochrome *cb*-type nitric oxide reductase with cytochrome *c* oxidase activity from *Paracoccus denitrificans* ATCC 35512. *J. Bacteriol. 178*, 1866–1871.

(45) Oubrie, A., Gemeinhardt, S., Field, S., Marritt, S., Thomson, A. J., Saraste, M., and Richardson, D. J. (2002)Properties of a soluble domain of subunit *C* of a bacterial nitric oxide reductase. *Biochemistry 41*, 10858–10865.

(46) Aasa, R., and Vanngard, T. (1975)EPR signal intensity and powder shapes: a reexamination. *J. Magn. Reson. 19*, 308–315.

(47) De Vries, S., and Albracht, S. P. J. (1979)Intensity of highly anisotropic low-spin heme EPR signals. *Biochim. Biophys. Acta 546*, 334–340.

(48) Saraiva, L. M., Besson, S., Fauque, G., and Moura, I. (1994) Characterization of the dihemic cytochrome c_{549} from the marine denitrifying bacterium *Pseudomonas nautica* 617. *Biochem. Biophys. Res. Commun. 199*, 1289–1296.

(49) Hendrich, M. P., and Debrunner, P. G. (1989)Integer-spin electron paramagnetic resonance of iron proteins. *Biophys. J. 56*, 489–506.

(50) Moenne-Loccoz, P., and de Vries, S. (1998)Structural characterization of the catalytic high-spin heme *b* of nitric oxide reductase: A resonance Raman study. *J. Am. Chem. Soc. 120*, 5147–5152.

(51) Hino, T., Matsumoto, Y., Nagano, S., Sugimoto, H., Fukumori, Y., Murata, T., Iwata, S., and Shiro, Y. (2010)Structural basis of biological N2O generation by bacterial nitric oxide reductase. *Science 330*, 1666–1670.

(52) Lachmann, P., Huang, Y., Reimann, J., Flock, U., and Adelroth, P. (2010)Substrate Control of Internal Electron Transfer in Bacterial Nitric-oxide Reductase. *J. Biol. Chem. 285*, 25531–25537.

(53) Rinaldo, S., Arcovito, A., Giardina, G., Castiglione, N., Brunori, M., and Cruruzzollà, F. (2008)New insights into the activity of *Pseudomonas aeruginosa cd*₁ nitrite reductase. *Biochem. Soc. Trans. 36*, 1155–1159.

(54) Ford, P. C., and Lorkovic, I. M. (2002)Mechanistic aspects of the reaction of nitric oxide with transition-metal complexes. *Chem. Rev. 102*, 993–1017.

(55) Cooper, C. E. (1999)Nitric oxide and iron proteins. *Biochim. Biophys. Acta 1411*, 290–309.

(56) Goodrich, L. E., Paulat, F., Praneeth, V. K. K., and Lehnert, N. (2010)Electronic structure of heme-nytrosyls and its significance for nitric oxide reactivity, sensing, transport, and toxicity in biological systems. *Inorg. Chem. 49*, 6293–6316 and references therein.

(57) Wang, Z.-Q., Wei, C.-C., and Stuehr, D. J. (2010)How does a valine residue that modulates heme-NO binding kinetics in inducible NO synthase regulate enzyme catalysis? *J. Inorg. Biochem. 104*, 349–356.

(58) Cordas, C. M., Pereira, A. S., Martins, C. E., Timoteo, C. G., Moura, I, Moura, J. J. G., and Tavares, P. (2006)Nitric oxide reductase: Direct electrochemistry and electrocatalytic activity. *ChemBioChem 7*, 1878–1881.

(59) Buschmann, S., Warkentin, E., Xie, H., Langer, J. D., Ermler, U., and Michel, H. (2010)The Structure of cbb(3) Cytochrome Oxidase Provides Insights into Proton Pumping. *Science 329*, 327–330.

(60) Hendriks, J. H., Prior, L., Baker, A. R., Thomson, A. J., Saraste, M., and Watmough, N. J. (2001)Reaction of carbon monoxide with the reduced active site of bacterial nitric oxide reductase. *Biochemistry 40*, 13361–13369.